Journal of the European Ceramic Society **6** (1990) 237–242

Synthesis of High Purity AlN by Nitridation of Li-Doped Al-Melt

Hermann Scholz & Peter Greil

Technische Universität Hamburg-Harburg, Arbeitsbereich Technische Keramik, D-2100 Hamburg 90, FRG

(Received 6 March 1990; revised version received 19 April 1990; accepted 25 April 1990)

Abstract

The isothermal nitridation of 2·3 wt% Li-doped Al-melt at 1273 K was investigated. Li promotes complete conversion of the Al to AlN and acts as a 'getter' reducing the oxygen impurities in the nitrogen atmosphere by forming $LiAlO_2$ and Li_2O. Thus, high-purity AlN powder could be obtained, containing low oxygen contamination (0·80 ± 0·02 wt%).

Die isotherme Nitridierung einer mit 2·3 Gew.% Li dotierten Al-Schmelze wurde bei 1273 K untersucht. Li fördert die völlige Umsetzung des Al zu AlN und gettert die Sauerstoffverunreinigungen in der Stickstoffatmosphäre durch die Bildung von $LiAlO_2$ und Li_2O. Auf diese Weise konnte hochreines AlN-Pulver mit einer geringen Sauerstoffverunreinigung von 0·80 ± 0·02 Gew.% gewonnen werden.

On a étudié la nitruration isotherme à 1273 K d'Al fondu dopé à 2·3% massiques de Li. Li facilite la conversion totale de l'Al en AlN et agit comme un piège pour les impuretés oxygène dans l'atmosphère azote en formant $LiAlO_2$ et Li_2O. On obtient ainsi une poudre d'AlN de haute pureté présentant une faible contamination en oxygène (0·80 ± 0·02% massique).

1 Introduction

Aluminium nitride ceramics are distinguished by their high thermal conductivity which may attain values up to 80%[1] of the theoretical value of 320 W/mK.[2] High density (>98% theoretical density) and low metallic (<200 ppm) and oxygen (<0·2 wt%) impurity contents, however, are required to minimize phonon scattering at intragranular crystal defects which are considered as the major limiting factor for thermal conductivity in AlN.[2–5] Thus, production of high-purity AlN-powder at low costs has become a key aspect for the development and future application of AlN-ceramics.

In contrast to the high-cost AlN fabrication routes, via the decomposition of Al halides (AlF_3, $AlCl_3$) and subsequent reaction with NH_3, carbothermal reduction of Al_2O_3 and the nitridation of solid Al-particles in N_2 or NH_3 are of particular importance for commercial AlN production. On pure Al a characteristic dense Al_2O_3 layer is adherent, even at room temperature.[6] At temperatures above 673 K a coherent AlN layer forms in nitrogen atmosphere which prevents further nitridation.[7] In order to attain complete nitridation of Al-particles at temperatures below the melting point, the average grain size has to be kept in the range of the thickness of the passivating AlN layer.[8] The following schematic relations summarize the production routes starting from solid ⟨Al⟩ or liquid {Al} reported in the literature:[9–12]

$$\langle Al\rangle + \tfrac{1}{2}(N_2) \xrightarrow{853K} \langle AlN\rangle \quad (1)$$

$$\{Al\} + \langle AlN\rangle + \tfrac{1}{2}(N_2) \xrightarrow{1423K} \langle AlN\rangle \quad (2)$$

$$\{Al\} + \tfrac{1}{2}(N_2/NH_3) \xrightarrow{1573K} \langle AlN\rangle \quad (3)$$

$$\{Al(Mg)\} + \tfrac{1}{2}(N_2) \xrightarrow{1473K} \langle AlN\rangle \quad (4)$$

$$\{Al(Zn)\} + \tfrac{1}{2}(N_2) \xrightarrow{1423K} \langle AlN\rangle \quad (5)$$

where ⟨ ⟩ denotes solid, { }, liquid and ( ) gaseous states of matter.

AlN obtained from nitridation of solid Al-particles with a mean grain size of 18 μm at 853 K according to reaction (1) exhibited residual Al

Journal of the European Ceramic Society 0955-2219/90/$3.50

contents of up to 10 wt% and oxygen contents of about 4 wt%. Higher temperatures impeded nitridation due to sintering of the metal powder. Nearly complete conversion to AlN and O_2 contamination of about 1·5 wt% was attained by mixing AlN with the Al-powder before nitridation at 1423 K (reaction (2)) in order to prevent sintering of the Al-particles.[9] Nitridation of pure Al at 1573 K in N_2 (5 vol.% NH_3) according to reaction (3) resulted in completely converted, highly reactive AlN-powder, which could be sintered to translucent AlN ceramics at 2173 K without any additional oxidic sintering aids.[10]

In accordance with the patented Lanxide™ process[13] the directed nitridation of molten Al necessitates initiating dopants to overcome the passivation effect of the dense AlN surface layer which forms on pure Al.[7] The influence of increasing Mg contents on the isothermal nitridation of Al at 1273 K (0·1 MPa) and the high-pressure nitridation (1473 K, 2 MPa) was studied in detail.[11,14] Under specific conditions a break-away nitridation could be achieved with complete conversion of Al to AlN. Corresponding to this mechanism Mg-doped Al[12] and Zn-doped Al[15] were proposed as precursors for low-cost fabrication of AlN (reactions (4) and (5)). Mg and Zn are supposed to be volatilized during the nitridation process due to the low evaporation temperature of these species ($T_e^{Mg} = 1380$ K, $T_e^{Zn} = 1180$ K at 0·1 MPa).

This paper deals with the effect of Li ($T_e = 1615$ K) as an alloying element on the melt nitridation of Al at 1273 K according to the reaction:

$$\{\text{Al(Li)}\} + \tfrac{1}{2}(N_2) \xrightarrow{1273\,K} \langle \text{AlN} \rangle \qquad (6)$$

Li is known to be one of the most surface active elements in Al[16] and initial experiments have shown that the nitridation of liquid Al is strongly accelerated by Li. In presence of oxygen impurities in the nitrogen atmosphere Li_2O or $LiAlO_2$ may preferentially form, so that Li may be considered as a 'getter' for oxygen. Thus, high-purity AlN reaction product can be expected from Al–Li-alloy melts.

2 Experimental

An Al-alloy containing 2·3 wt% Li (Metallhüttenkunde, RWTH-Aachen, FRG) and metallic impurities (Si, Fe, Cu, Mg, Zn, Ti) of <0·01 wt% was prepared for the nitridation experiments. Cylindrical specimens of 15 mm in diameter and 9 mm in height were machined and ultrasonically cleaned in acetone and finally placed in alumina crucibles. Isothermal nitridation at 1273 K for 5 h was carried out in a resistance-heated Al_2O_3 tube furnace (Hochtemperaturtechnik, Saarbrücken, FRG) under flowing nitrogen (99·999% N_2, major impurities: 5×10^{-4} vol.% H_2O, 3×10^{-4} vol.% O_2). The nitridation experiments were restricted to only this single temperature because preliminary experiments showed complete conversion of Al to AlN without significant Al evaporation (<0·6 wt%), although higher temperatures might be possible. Similar experiments with Mg- and Si-doped Al-alloys provided information on the behavioural transition between different reaction mechanisms at this temperature as a function of the alloy composition and the oxygen content in the nitriding atmosphere.[14] After evacuation to $<10^2$ Pa the chamber was refilled with nitrogen three times at 423 K in order to remove traces of atmospheric oxygen and water. A constant heating rate of 5 K/min was applied from 423 K up to the isothermal nitridation temperature of 1273 K. The temperature was measured by Pt/Pt–10% Rh thermocouples. During nitridation in N_2 atmosphere of 0·1 MPa flow rates of 0·2 litre/min (tube furnace) and 0·03 litre/min (thermobalance) were applied. Smaller samples of 5 mm in diameter and 5 mm in height were examined in a thermobalance (STA 409, Netzsch, Selb, FRG). Thermal, atmospheric and pressure conditions were analogous to those used in the tube furnace.

The reaction product was analysed by X-ray diffraction (PW 1729, Philips, Netherlands) using monochromated $Cu_{K\alpha}$-radiation and scanning electron microscopy (JSM 840 A, Jeol, Japan) with ultrathin window and energy dispersive spectroscopy. The oxygen content was determined by combustion with excessive carbon and subsequent measurement of heat conductivity of the oxygen-containing gas (TC-136, LECO Corp., USA). The Li content was analysed by flame emission spectroscopy (PE-2380, Perkin-Elmer, USA) of the specimen powder dissolved in NaOH solution.

Phase equilibria were calculated with the thermodynamic program system equiTherm (VCH Verlagsgesellschaft mbH, Weinheim, FRG)[17] in order to evaluate the influence of Li on the nitridation of Al in presence of O_2 impurities. The program calculates the equilibrium composition of condensed and gas-phase mixtures based on the method of free energy minimization.[18] Six condensed and six gaseous substances in the system Li–Al–O–N were considered in the calculations, the thermodynamic data of which are given in Table 1.[19] The results of the phase equilibria calculations are presented as isothermal

Table 1. Standard Gibbs energies of formation of the phases considered in the Al–Li–N–O system at 1273 K[19]

Condensed species	$\Delta_f G°$(*kJ/mol*)
Al	0
AlN	−179·750
Al_2O_3	−1 271·125
Li	0
Li_2O	−429·315
$LiAlO_2$	−913·086
Gaseous species	$\Delta_f G°$(*kJ/mol*)
Al	+165·689
Al_2O	−235·152
Li	+31·599
Li_2O	−228·329
O_2	0
N_2	0

phase amount diagram for the initial Al-alloy composition showing the proportions of condensed phases in a mixture for a range of O_2 concentrations in the reaction gas (N_2) atmosphere.

3 Results

Li as an alloying element considerably changes the nitridation behaviour of molten Al at 1273 K in N_2. Whereas pure Al forms a thin, protective AlN layer on the surface which inhibits further nitridation, the Li-doped (2·3 wt%) Al provokes a combustion-like breakaway nitridation with 100% conversion of Al to AlN. Figure 1 shows the weight gain of the Al-melt during isothermal nitridation in flowing N_2 (0·03 litre/min) at 1273 K. In contrast to the nitridation of Mg-doped Al-melts[14] a very short incubation period of approximately 40 min occurred and complete conversion to AlN is achieved after 100 min. Maximum conversion rates of 1 wt%/min

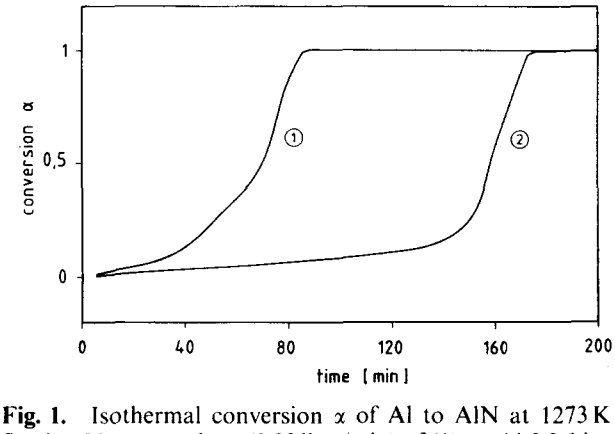

Fig. 1. Isothermal conversion α of Al to AlN at 1273 K in flowing N_2 atmosphere (0·03 litre/min) of (1) an Al 2·3 Li-melt compared to (2) Al 2·5 Mg-melt.[12]

were determined, which is in the range of reaction rates found for 2·5 wt% Mg-doped Al. The total weight gain of Al equals 52 wt% which corresponds to a conversion ratio $\alpha = 1$, calculated according to the equation:

$$\alpha = M_{Al}/M_N \cdot (m_{rp} - m_{Al}) \quad (7)$$

M denotes the molecular and m the actual weight of the indexed elements (Al, N) and the reaction product (rp). Li can be neglected because the total content of residual Li in the reaction product was analysed to be less than the detection limit of 0·05 wt%. XRD analysis only revealed AlN of high purity. The lattice parameter deviation was $< 0{\cdot}00015$ nm according to JCPDS data (Card No. 25-1133) which points to very low oxygen contents dissolved in the AlN lattice.[20] The total amount of adsorbed and dissolved oxygen was determined to be $0{\cdot}80 \pm 0{\cdot}02$ wt%.

The as-nitrided reaction product consists of a porous compact with a white friable bulk and a plane, hard surface of black colour. In contrast to the nitridation of Al–Mg-alloys[14] no wetting of the crucible walls occurred and high reproducibility was achieved. Two different morphologies of AlN reaction products were observed: (i) crystals of predominant globular morphology with a mean grain diameter of ≈ 1 μm (Fig. 2(a)) and (ii) elongated crystals of needle-like shape orientated perpendicular to the growth surface (Fig. 2(b)). The elongated AlN crystals were found in the upper parts of the reaction product and may have formed at higher temperatures,[21] due to the highly exothermic AlN formation reaction ($\Delta_f H°_{1273K} = -329{\cdot}136$ kJ/mol).[22] The appearance of well-faceted grains and pore morphologies and a significantly larger grain size of 2–10 μm indicates the onset of sintering and grain growth of the AlN-reaction product (Fig. 2(c)), resulting in higher hardness compared to the friable bulk. From the residual pores large dihedral angles ($\approx 120°$) may be seen at the grain boundaries.

4 Discussion

In contrast to the passivation effect of dense surface layers, a surface active nitridation was observed in Al(Mg,Si)-alloys which is characterized by a continuously growing nitride layer typically containing 5 to 25 vol.% of residual Al.[13] Based on the enhanced nitridation behaviour of liquid Al-alloys a novel fabrication process of AlN/Al ceramic–metal composites (CMC) called directed melt oxidation

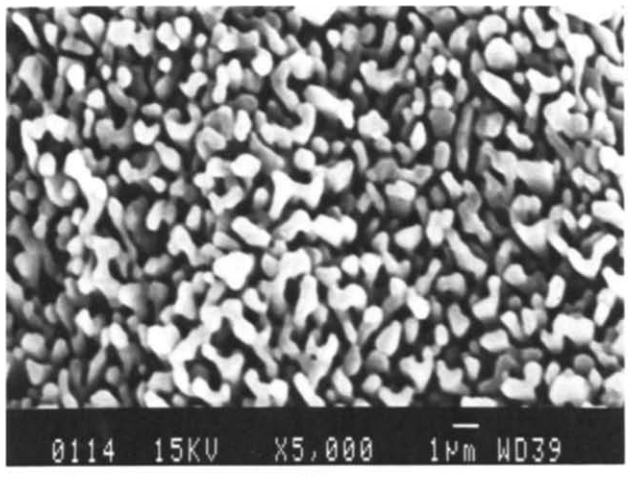

(a)

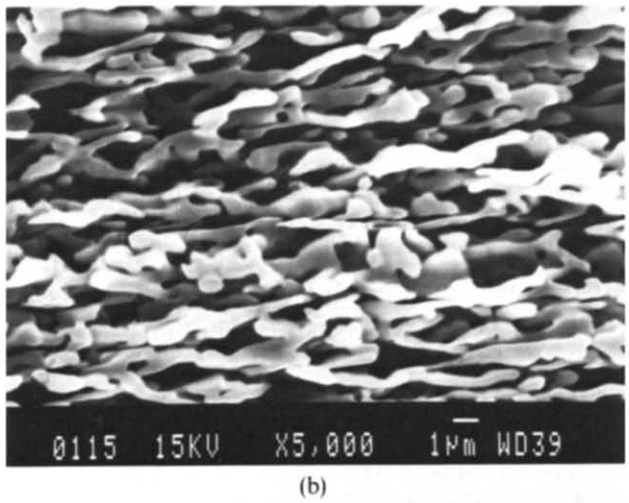

(b)

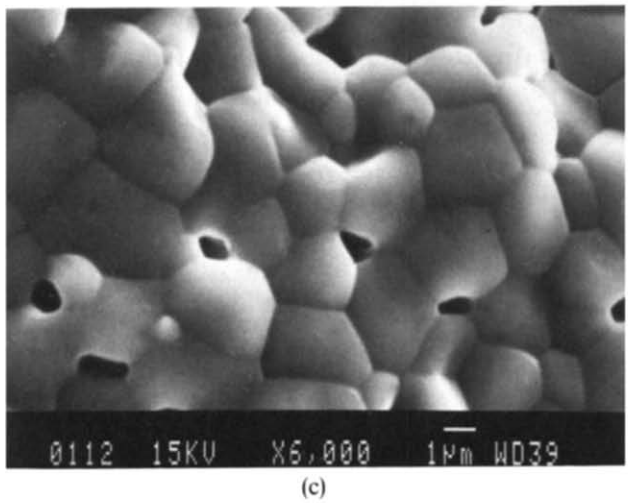

(c)

Fig. 2. SEM micrographs of (a) and (b) molten metal derived AlN fractured surface and (c) as-grown surface.

(DIMOX, Lanxide™ process) was developed in analogy to the Al_2O_3/Al materials.[23] It could be shown, however, that with increasing Mg/Si ratio and decreasing O_2 content in the nitriding atmosphere four major reaction mechanisms may be separated:[14] (i) a passivating surface nitridation, (ii) a volume nitridation with precipitation of isolated AlN in the Al matrix, (iii) a volume nitridation resulting in a three-dimensionally interconnected AlN/Al composite microstructure (Lanxide type) and (iv) a breakaway nitridation with complete conversion of Al to AlN. The behavioural transition of the nitridation mechanism is reflected by the growth direction and crystal morphology of AlN which change from inward (mechanisms (i) and (ii)) to outward (mechanisms (iii) and (iv)) growth of the reaction product with [0001] as the dominating growth direction.

In correspondence to the Mg- and Si-containing Al-melt nitridation where Mg was considered to act as an oxygen 'getter' over the melt surface and thereby reducing the partial pressure of oxygen, Li may exert a similar effect on the nitridation behaviour of binary Al(Li)-melt. The low residual oxygen ($0{\cdot}80 \pm 0{\cdot}02$ wt%) and lithium ($<0{\cdot}05$ wt%) contents in the AlN reaction products may therefore be explained in terms of the phase equilibria that develop as a function of the oxygen content in the nitriding atmosphere. The thermodynamic calculations show AlN to be the major condensed phase in the Al–Li–O–N system at oxygen contents $<0{\cdot}1$ vol.% in the N_2 reaction gas (Fig. 3(a)). According to the phase equilibria calculations the oxygen will be preferentially 'gettered' by Li, resulting in the formation of Li_2O at low and $LiAlO_2$ at higher oxygen concentrations:

$$2\{Li\} + \tfrac{1}{2}(O_2) \longrightarrow \langle Li_2O \rangle$$
$$\Delta_f G^\circ_{1273K} = -429{\cdot}315\ \text{kJ/mol} \quad (8)$$

$$\{Li\} + \{Al\} + (O_2) \longrightarrow \langle LiAlO_2 \rangle$$
$$\Delta_f G^\circ_{1273K} = -913{\cdot}086\ \text{kJ/mol} \quad (9)$$

The partial pressure calculations of the major gaseous phases in the Li–Al–O–N system (Fig. 3(b)) show Li as the dominating gaseous species with a partial pressure 7–12 orders of magnitude higher than Al. Due to the consumption of oxygen by reactions (8) and (9) the oxygen partial pressure becomes extremely low ($p_{O_2} < 10^{-25}$ Pa below $c_{O_2} <$ 1 vol.%) resulting in the presence of elemental Li to be in equilibrium with AlN at $c_{O_2} < 10^{-3}$ vol.% (Fig. 3(a)).

Volatilization of Li and Li_2O may further contribute to the depletion of residual Li in the reaction product. The possible reactions involving gaseous reaction products in the Li–O system are:

$$\{Li\} \longrightarrow (Li)$$
$$\Delta_f G^\circ_{1273K} = 31{\cdot}565\ \text{J/mol} \quad (10)$$

$$2\{Li\} + \tfrac{1}{2}(O_2) \longrightarrow (Li_2O)$$
$$\Delta_f G^\circ_{1273K} = -228\,395\ \text{J/mol} \quad (11)$$

$$\langle Li_2O\rangle \longrightarrow 2\{Li\} + \tfrac{1}{2}(O_2)$$
$$\Delta_f G^\circ_{1273K} = 429\,315\ \text{J/mol} \qquad (12)$$

$$\langle Li_2O\rangle \longrightarrow 2(Li) + \tfrac{1}{2}(O_2)$$
$$\Delta_f G^\circ_{1273K} = 492\,445\ \text{J/mol} \qquad (13)$$

$$\langle Li_2O\rangle \longrightarrow (Li_2O)$$
$$\Delta_f G^\circ_{1273K} = 200\,920\ \text{J/mol} \qquad (14)$$

From the volatility diagram[24] constructed from eqns (10)–(14) (Fig. 4) gaseous Li and gaseous Li_2O are suggested to become stable at the calculated partial pressures of oxygen and the Li and Li_2O phases, respectively. Because of the flowing nitrogen gas stream the evaporated gas species will be removed from the specimen site so that no equilibrium may be generated. Thus, a significantly higher mass flow, as it would be expected in the case of stable equilibrium condition, will develop, which may further contribute to the depletion of the residual Li content. Significantly higher vapour pressure of Li and Li_2O as compared to Al combined with low oxygen solubility in the Al-melt ($c_{O_2} <$ 50 ppm at 1273 K[25]) will cause the reaction to occur on the melt surface, which is confirmed by XRD-analysis showing γ-$LiAlO_2$ precipitated on the specimen surface. Thus, in-situ purification of Li-doped Al-melt during nitridation of Al may be achieved due to oxygen 'gettering' by Li and removal of the gaseous reaction products from the reaction site.

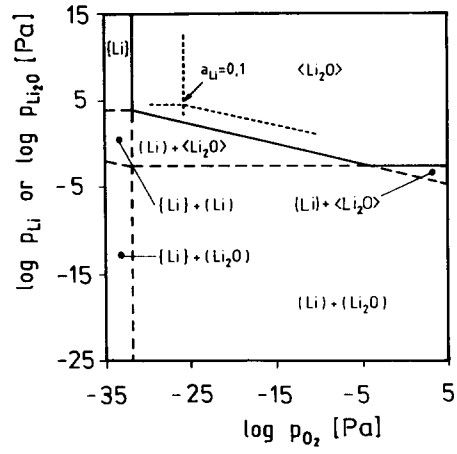

Fig. 4. Volatility diagram for the Li–O system at 1273 K ($a_{Li} = 1$) constructed according to reactions (10) to (14).

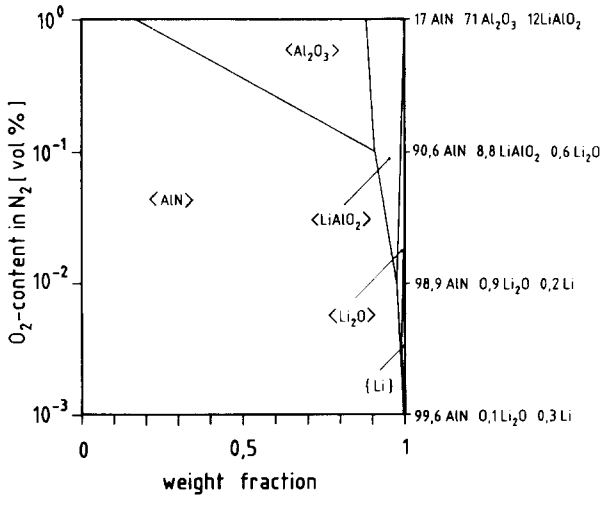

(a)

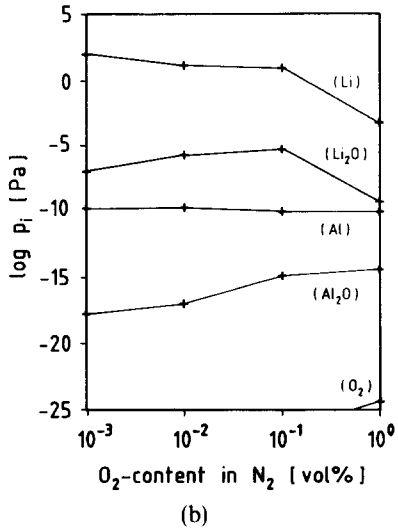

(b)

Fig. 3. (a) Isothermal phase amount diagram of the condensed phases and (b) partial pressures of the gaseous species at 1273 K in the system Al–Li–O–N for the alloy composition Al:2·3 Li as a function of the O_2-content in the nitriding atmosphere.

As may be seen from Fig. 1 the reaction kinetics of both the Mg/Si- and Li-containing Al-alloys are characterized by an induction period with a slowly increasing reaction rate followed by a rapid increase of Al to AlN conversion. The incubation period may be attributed to the nucleation of AlN on the melt surface which is followed by the directed growth of the AlN-crystals, as was concluded from kinetics data analysis in Mg/Si-doped Al.[14] Due to the lower atomic weight and higher surface activity of Li in Al as compared to Mg,[16] however, the nucleation period in Li-doped Al may be shorter. In contrast to the controlled nitridation and growth of the dense AlN/Al layer according to the Laxide™ process (mechanism (iii)), the friable reaction product of the rapid nitridation shows a highly porous microstructure with a high specific surface of the AlN grains (Fig. 2(a) and (b)). A linear growth of the highly porous AlN crystals perpendicular to the initial melt surface can be concluded from Fig. 2(b). The Al-melt may easily be transported to the reaction site via the AlN surface and open channels. Only at extremely low O_2 content in the nitriding atmosphere due to the presence of 'getter elements' like Mg or Li enhanced wetting of the Al-alloys provides a high reaction surface which seems to be a

presupposition for initiating and maintaining the breakaway nitridation with rapid melt transport to the reaction site. Hence, by change of the nitriding atmosphere composition volatilization of Li may be controlled, which may be used to optimize nitridation kinetics and microstructure formation. In contrast to the Lanxide™ process, where the nitridation process is controlled by the amount of alloying elements in the Al-melt, additional control of the O_2 content in the nitriding atmosphere allows the reaction kinetics to be influenced throughout the whole reaction process.

5 Conclusions

AlN-powder with low oxygen content of $<0{\cdot}81$ wt% could be obtained from Li-doped Al-melt in an unpurified nitrogen atmosphere. Li is supposed to act as a 'getter element' for oxygen contamination. Hence internal (Li content in Al) or external (O_2 content in N_2) control of the nitridation reaction and product purity may be achieved. Thus, AlN-powders with various powder morphologies and purities may be produced at high reaction rates and temperatures of about 1273 K. Using commercial Al–Li-alloys which have been developed for applications in aerospace constructions the melt nitridation process may represent an interesting alternative for the production of high-purity AlN at moderate costs.

Acknowledgement

Mr Adler of the University of Erlangen–Nuernberg is gratefully acknowledged for the oxygen measurements.

References

1. Kurokawa, Y., Hamaguchi, H., Shimada, Y., Utsumi, K. & Takamizawa, H., Highly thermal conductive AlN-substrates. In *Proc. Int. Symp. Microelectr.*, 1987, p. 654.
2. Slack, G. A., Nonmetallic crystals with high thermal conductivity. *J. Phys. Chem. Solids*, **34** (1973) 321.
3. Slack, G. A., Tanzilli, R. A., Pohl, R. O. & Vandersande, J. W., The intrinsic thermal conductivity of AlN. *J. Phys. Chem. Solids*, **48** (1987) 641.
4. Kranzmann, A. E., Wärmeleitfähigkeit von drucklos gesinterten AlN-Substratkeramiken. PhD thesis, University of Stuttgart, FRG, 1988, in German.
5. Sakai, T., Kuriyama, M., Inukai, T. & Kizima, T., Effect of the oxygen impurity on the sintering and the thermal conductivity of AlN polycrystal. *J. Ceram. Soc. Jpn*, **86** (1978) 174.
6. Thiele, W., Oxydation von Al- und Al-Legierungsschmelzen. *Aluminium*, **38** (1962) 780.
7. Long, G. & Foster, L. M., AlN—a Refractory for Al to 2000°C. *J. Am. Ceram. Soc.*, **42**(2) (1959) 53.
8. Jelacic, C. & Petrovski, P., Cinetica della nitrurazione dell' Al e delle leghe Al–Si in N_2 e NH_3. *La Ceramica*, **31**(4) (1978) 17.
9. Belau, A. & Müller, G., Nitridation of Al-powders near by the melting temperature of the metal. *cfi/Ber. DKG*, **65**(5) (1988) 122.
10. Kimura, I., Ichiya, K., Ishii, M., Hotta, N. & Kitamura, T., Synthesis of fine AlN powder by a floating nitridation technique using an N_2/NH_3 gas mixture. *J. Mater. Sci. Lett.*, (8) (1989) 303.
11. Schweighofer, A. & Kudela, S., High-pressure nitridation of AlMg alloys. *Kovove Materialy*, **15**(3) (1977) 257.
12. Kudela, S. & Schweighofer, A., Czechoslovakian Patent No. 189 513, 1978.
13. Creber, D. K., Poste, S. D., Aghajanian, M. K. & Claar, T. D., AlN-composite growth by nitridation of Al-alloys, *Ceram. Eng. Sci. Proc.* **9**(7–8) (1988) 975.
14. Scholz, H. & Greil, P., Nitridation reactions of molten Al–(Mg, Si)-alloys. *J. Mater. Sci.* (1990) (in press).
15. van Dam, Ir. M., Philips Gloeilampenfabrieken/Eindhoven, Patent No. 6602899, 1966.
16. Lang, G., Einfluß von Zusatzelementen auf die Oberflächenspannung von flüssigem Reinstaluminium. *Aluminium*, **50**(11) (1974) 731.
17. Zeitler, M., Wittig, B. & Schmidt, W., equiTherm, VCH Wissenschaftl. software, 1989.
18. Eriksson, G., Thermodynamic studies of high-temperature equilibria. *Chem. Scripta*, **8** (1975) 100.
19. Barin, I., *Thermochemical Data of Pure Substances*. VCH Verlagsgesellschaft, Weinheim, FRG, 1989.
20. Slack, G. A., McNelly, T. F., Growth of high-purity AlN crystals. *J. Crystal Growth*, **34** (1976) 263.
21. Choi, S. W. & Lee, S. J., Synthesis of AlN from metal Al powders. *J. Korean Ceram. Soc.*, **22**(6) (1985) 80.
22. Chase, M. W., Davies, C. A., Downey, J. R., Frurip, D. J., McDonald, R. A. & Syverud, A. N., *JANAF Thermochemical Tables*, 3rd edn, J. Phys. Chem. Ref. Data, Vol. 14, Suppl. 1, 1985.
23. Newkirk, M. S., Urquhart, A. W., Zwicker, H. R. & Breval, E., Formation of Lanxide™ ceramic composite materials. *J. Mater. Res.*, **1** (1986) 81.
24. Lou, V. L. K., Mitchell, E. & Heuer, A. H., Review—graphical displays of the thermodynamics of high-temperature gas–solid reactions and their application to oxidation of metals and evaporation of oxides. *J. Am. Ceram. Soc.*, **68**(2) (1985) 49.
25. Hansen, M., *Constitution of Binary Alloys*, 2nd edn, McGraw-Hill, New York, 1958.